Soil-Water Characteristics and Creep Deformation of Unsaturated Expansive Subgrade Soil: Experimental Test and Simulation

Yongsheng Yao[1], Jue Li[1]*, Ziqiong Xiao[2] and Hongbin Xiao[3]

[1]College of Traffic and Transportation, Chongqing Jiaotong University, Chongqing, China, [2]School of Economics, Central South University of Forestry and Technology, Changsha, China, [3]School of Civil Engineering, Central South University of Forestry and Technology, Changsha, China

The creep deformation of expansive soil has been considered as a vital threat to the safety in engineering construction because it may cause serious slope diseases in geological engineering. Meanwhile, since expansive soil usually remains in unsaturated state, its mechanical property is significantly affected by the seasonal environment. Therefore, the nonlinear deformation of expansive soil has received increasing attention, especially the humidity-dependent creep properties. This study focused on the stability of the unsaturated expansive soil subgrade considering rainfall and the creep behavior. Pressure plate extractor and direct shear tests were performed to investigate the hydro-mechanical and creep characteristics of the unsaturated expansive soil. Both the Van-Genuchten and Burgers models were applied to analyze the test results and inserted into the numerical model of the slope under rainfall infiltration. Results show that the compaction degree and the stress state was closely related to the water holding capacity of the expansive soil. The nonlinearity of the creep behavior became increasingly obvious with the increase of time and the stress level. The safety factor of the slope decreased as the rainfall time increased, and the most dangerous slide of the slope moved toward the foot of the slope. Considering the long-term creep process, there was a period of rapid growth in horizontal displacement that is detrimental to the stability of the slope. Besides, the rainfall infiltration could accelerate the slope failure before and after this creep process.

Keywords: subgrade engineering, expansive soil, soil-water characteristics, creep behavior, numerical simulation

1 INTRODUCTION

Disasters caused by expansive soil have received increasing attention with the development of engineering construction (Ikeagwuani and Nwonu, 2019). Expansive soil is a special kind of porous soil with moisture dependence and is rich in kaolinite, montmorillonite, illite, and other mineral components (Leng et al., 2018). The repeated swelling and shrinking behavior of expansive soil is caused by the change in natural environment (Soltani et al., 2018). For example, under the drying and wetting cycles, the overlying pavement with expansive soil will be prone to uneven settlement, leading to the destruction or instability of the engineering structure (Lu et al., 2019). This phenomenon presents significant challenges to road engineering in designing and building stable

pavement structures (Khan et al., 2020). Expansive soil is widely distributed in more than 40 countries and regions. In China, the annual economic loss caused by the geological disasters caused by expansive soil is as high as 15 billion. Current studies show that the expansive soil slope has the characteristics of shallow layer expansion and contraction and seasonality (Mehta et al., 2017). The soil–water characteristics of expansive soil are closely related to its strength. In pavement engineering, the most expansive soil subgrade structures are located above the groundwater level and remain in unsaturated state for a long time. Zhang et al. (2020) analyzed the water–air migration law of the subgrade structure through a series of numerical models and found that, considering the atmospheric environment, groundwater, and other factors, the water content of subgrade soil gradually increases during the operation period and reaches the equilibrium state in approximately 3 years. However, the current traditional framework used for pavement design and construction ignores the water migration law and its effect on unsaturated embankment soil.

The hydraulic characteristics of expansive soils are fully understood by the soil–water characteristic curve (SWCC). SWCC is an important testing tool to investigate the relationship between matric suction and water content of the unsaturated soil (Yao et al., 2019). Li et al. (2019) emphasized that it is necessary for subgrade design to establish the humidity field affecting the stiffness and deformation of the subgrade structure. It is widely accepted that matric suction plays an important role in mechanical properties of the unsaturated soil, including resilient modulus and shear strength (Yao et al., 2018). Pooni et al. (2021) applied the dewpoint potentiometer to measure the hydraulic behavior and the results showed the hydraulic variation has strong influence on the stabilization for an expansive subgrade. Therefore, the SWCC features of expansive soil must be investigated to scientifically and effectively evaluate the stability of the expansive soil slope (Dai et al., 2020). In general, matric suction can be measured directly or indirectly. Direct measurement can be performed using the tensiometer (Take and Bolton, 2003), axis-translation (Toll et al., 2013), and filter paper (Houston et al., 1994) methods. The pressure plate extractor has been widely utilized in assessing the SWCC of unsaturated soil on the basis of axial translation technology (Wang et al., 2015). A clay plate is used in this device with a high air intake value to isolate the gas and water phases in the soil to achieve precise suction control. Meanwhile, some mathematical models have been proposed by fitting the test data points into continuous functions to describe the SWCC behavior (Yang and Bai, 2019). Fredlund and Xing (1994), Van Genuchten (1980) and Gardener et al. (1970) have all made outstanding contributions in these models. Among them, the Van-Genuchten model is considered to have a good fitting effect and reliability and has been widely used to predict the permeability coefficient, strength, and pore water distribution of unsaturated soils.

In addition to the soil–water characteristics, the rheological property of the expansive soil is also considered in slope stability (Cong et al., 2020). The rheological behavior study mainly focuses on the creep deformation of expansive soil over time (Pawlik and

TABLE 1 | Physical soil properties.

| Index	Testing value
Natural moisture content (%)	26.5
Density (g/cm^3)	1.93
Void ratio	0.77
Specific gravity	2.70
Saturation (%)	92.9
Liquid limit (%)	61.4
Plastic limit (%)	22.8
Plasticity index (%)	38.6
Maximum dry density (g/cm^3)	1.89
Optimum moisture content (%)	15.8
Free expansion ration (%)	62.5

Šamonil, 2018). In terms of the creep test, the research object covers a wide range, such as coarse–grained (Hou et al., 2018), marine sediment (Huang et al., 2020), and frozen (Li et al., 2017) soils. Given its high water content and compressibility, soft soil has an obvious creep characteristic (Zhou et al., 2021). Many studies have been conducted on the creep characteristics of soft soil. However, for hard clays, such as expansive soils, few studies have been conducted on the creep properties (Shan et al., 2021). As the key to solving the creep-related problems of expansive soil, a constitutive model of creep behavior is developed to discuss the relationship between deformation, stress, strength, and time (Liu et al., 2020). According to the experimental test data, some researchers established the theoretical creep model by using mechanical theory and element combination. Fan et al. (2011) carried out compression creep tests and compared the Burgers and K-H models by fitting the rheological properties of expansive soil. Peng et al. (2020) found that the nonlinear fractional derivative creep model could describe the creep characteristics of expansive soil well and established a shear creep constitutive equation and its parameters. Therefore, the creep mechanism of expansive soil must be explored, and the theoretical model must be introduced in practical engineering design to fundamentally control the disasters caused by expansive soil.

In previous research, the numerical method was usually applied to analyze the failure mechanism of slopes and was supported by experimental results (Zheng et al., 2018; Zheng et al., 2021). It is a responsible way to quickly predict the stability of slopes under different environmental and loading conditions. Therefore, the moisture distribution of an expansive soil slope in this study was calculated using the Geo-studio software and inserted into the FLAC3D model. The study aims to evaluate the stability of the unsaturated expansive soil subgrade using the rainfall infiltration model and consider the creep deformation. Thus, experimental tests were performed to investigate the hydro-mechanical characteristics of unsaturated expansive soil and survey the influences of compaction and stress on the SWCC results. Similarly, the creep behavior of expansive soils was studied using direct shear tests, and the results were fitted by the Burgers model. In the simulation, the non-linearity and time dependence of the shear properties were defined by the CVISC creep model.

TABLE 2 | Mineral properties of expansive soil.

Mineral composition (%)	Expansive soil
Montmorillonite	10–15
Hydromica	15–25
Quartz	20–30

saturation or volume and water content in unsaturated soils. SWCC is commonly used to characterize the water holding capacity of unsaturated soils and is influenced by several factors, including mineral composition, grain size distribution, overlying stress, and dry density. Therefore, SWCC and its
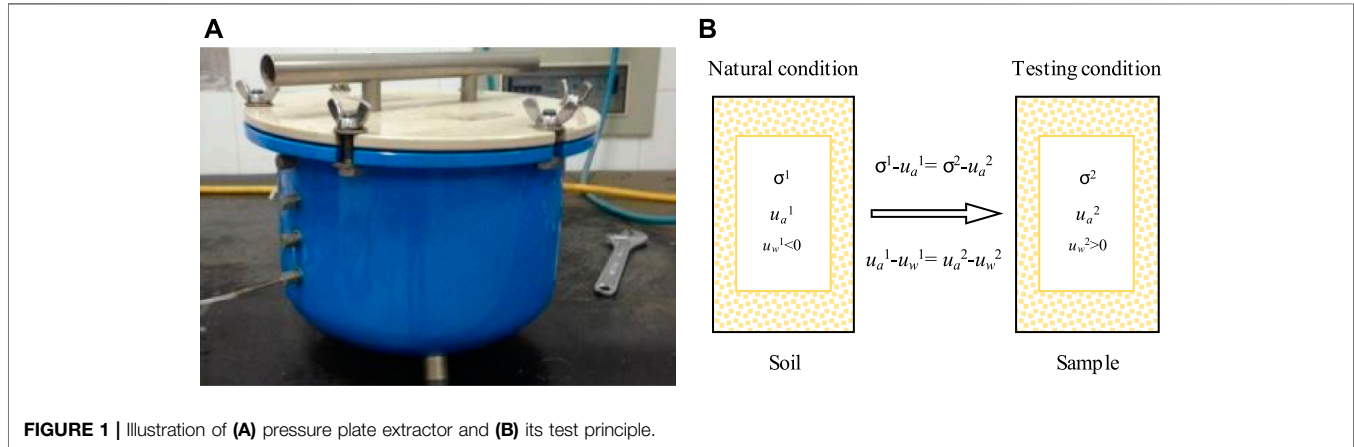
FIGURE 1 | Illustration of (A) pressure plate extractor and (B) its test principle.

2 MATERIALS AND METHODS

2.1 Materials

The soil samples were taken from Nanning, Guangxi, from alluvial expansive soil. Physical property and XRD diffraction tests were carried out on the soil samples. The basic physical property index and the mineral composition are shown in **Tables 1**, **2**.

The mineral composition and content are one of the important factors affecting the mechanical properties of expansive soil. Generally, the higher the content of strong hydrophilic minerals (such as montmorillonite hydromica) in the soil is, the greater the water absorption rate of the soil and the higher the plasticity index are. In particular, the relaxation rate of the soil samples and the significance of the creep characteristics of the test results increase with montmorillonite content. Quartz has little effect on stress relaxation.

Some studies show that the expansive soil in the subgrade slope gradually evolves into the sheet frame or stack structure after long-term compression (Jalal et al., 2020). The results show that the shear creep characteristic is obvious. In addition, after expansive soil absorbs water, the thickened structural water film on the surface of the soil particles increases the viscosity between the soil particles, which leads to the more obvious creep characteristics of expansive soil. Therefore, SWCC and direct shear creep tests must be performed on expansive soil to understand the engineering properties of the expansive soil subgrade.

2.2 Soil–Water Characteristic Curve Test

SWCC is a concept introduced by soil hydrodynamics and is defined as the curve of the relationship between suction and

prediction model are among the natural characteristics of expansive soil.

The pressure plate extractor Model1600-15bar produced by the Soil Moisture Company of the United States was used in this test, as shown in **Figure 1A**. The test device adopts shaft translation technology to control the suction to avoid the gasification of water in the suction control system. The technique achieves a positive pore water pressure (u_w) by increasing the pore gas pressure (UA). As shown in **Figure 1B**, the total stress (σ^1), pore gas pressure (u_a^1), and pore water pressure (u_w^1) of unsaturated soil under natural conditions increased to σ^2, u_a^2, and u_w^2 during the process of compression. However, the net normal stress (σ-u_a) and matric suction (u_a-u_w) of the tested soil samples did not change. Consequently, the pressure plate meter enables the control of matric suction at high atmospheric pressures. Zhang et al. (2021) studied the water-holding performance of the typical subgrade soil, and their results show that the matric suction is generally in the range of 0–1,000 kPa. Given that the maximum control suction of the 15Bar clay plate reaches 1,500 kPa, this test meets the SWCC test requirements of unsaturated expansive soil. The main test procedures are as follows.

(1) The clay plate is fully saturated. The pressure chamber is filled with distilled water until the clay plate is submerged by 1–2 cm. The pressure chamber and valve are closed to apply a pressure of 5 kPa. The clay plate reaches saturation until the volumetric flask is free of bubbles.

(2) The saturated soil sample is installed in the pressure chamber. The ring knife sample of expansive soil reaches the saturation state through the vacuum method. A saturated

Vertical stress (kPa)	Shear stress (kPa)
50	8.5 → 25.5 → 42.5 → 93.5 → 161.5
100	8.5 → 25.5 → 42.5 → 93.5 → 161.5
200	8.5 → 25.5 → 42.5 → 127.5 → 204
300	8.5 → 25.5 → 42.5 → 127.5 → 204

soil sample is placed on a clay plate, and the pressure chamber is closed. The internal pressure is adjusted to 0.1 kPa for the soil sample to reach equilibrium. The balance of the soil sample is marked by the absence of change in mass or water flow from the drain.

(3) The water content of the soil sample is calculated using the mass method. The mass of the balanced soil sample is measured using an electronic balance (with an accuracy of 0.001 g).

(4) The above process is repeated to obtain the water content under different suction forces. The corresponding water content is tested under a series of suction conditions (1, 10, 20, 50, 100, 200, 400, 800, and 1,000 kPa), and the corresponding SWCC curve is drawn.

2.3 Direct Shear Creep Test

An improved stress-controlled direct shear instrument, made in Nanjing, China, was used for testing. This experiment aims to obtain the relationship between the strain and time of expansive soil under different stresses. Two kinds of loading methods can be used for the creep test on soil, including separate and graded loading. At present, the graded loading method is often used, that is, the same sample is tested under different stress levels. The method does not have significant differences in soil samples and instruments, thus ensuring a small dispersion in test data. Therefore, the hierarchical loading method was adopted in this study. Shear creep tests were carried out at four vertical stresses (50, 100, 200, and 300 kPa), and the test sequence is shown in **Table 3**. The test procedure is as follows.

(1) The specimen is unsaturated and consolidated under specified stresses. To prevent moisture evaporation in the soil samples during consolidation, a wet cloth covers the shear box.

(2) Rapid shear test is performed on the consolidated soil samples. The shear rate is 12 RPM, and the peak shear strength under different stresses is measured. As shown in **Table 3**, the maximum shear stress for each stage loading is determined.

(3) The shear strain is obtained by stepwise loading. According to the sequence in **Table 3**, horizontal shear stress is applied to the soil samples. The next load is applied after the strain stabilizes.

3 NUMERICAL MODELLING METHODOLOGY

Rainfall infiltration is a complex saturation-unsaturation seepage process. This process causes changes in the pore water pressure,

volume, water content, and transient saturated zone of the expansive soil slope (Yao et al., 2021). These changes are detrimental to slope stability. Therefore, finite element analysis was carried out under rainfall conditions to capture the deformation behavior of unsaturated slopes to evaluate the effectiveness of stability, further illustrating the importance of SWCC for the structural design of subgrade soil. Meanwhile, the humidity of the subgrade also affects the creep characteristics of the expansive soil slope. In this paper, combined with the built-in CVISC constitutive model, the influence of the superposition effect of humidity and creep on the deformation of an expansive soil slope is discussed.

3.1 Slope Geometry and Parameters

A typical expressway slope in Nanning was selected for numerical modeling, as shown in **Figure 2**. The height of the clay slope is 10 m, and the slope ratio is 1:2.0. Geological exploration revealed that the shallow layer of the slope is expansive soil (0–2 m), and the lower layer is pluvial clay. The physical parameters of each layer of soil were assumed constant, and the contact of each layer is a fully connected. **Table 4** summarizes the material properties of each soil layer. The initial humidity of the slope is considered uniform and constant, and the water table is located 1.5 m above the bottom of the model. The hydraulic characteristics of the soil layer are discussed in the next section.

3.2 Numerical Simulation of Rainfall Process

Geo-studio was used for the numerical simulation of the slope to simulate the hydraulic response of expansive soil and the slope stability under the condition of rainfall. The SEEP/W module of this software accurately simulated the seepage process of saturated unsaturated soil through the Richards governing equation. To deal with the severe hydraulic response caused by water seepage at the boundary, the quadrilateral element with vertical joints was used to discretely treat the shallow expansive soil in the model. Other areas used the mixed regular quadrilateral and triangle elements. The surface of the
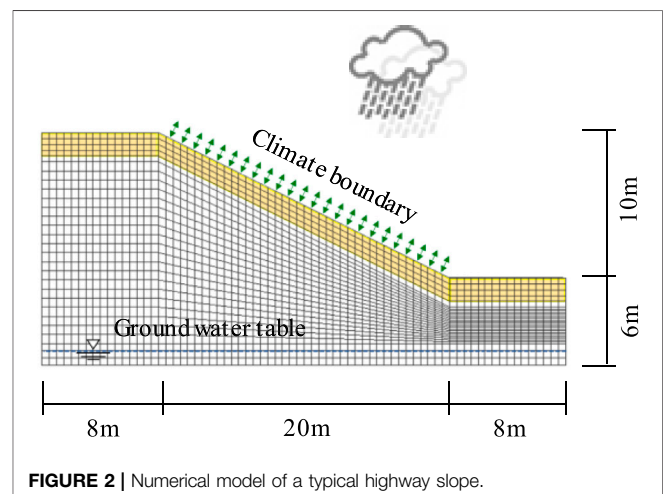
FIGURE 2 | Numerical model of a typical highway slope.

TABLE 4 | Material properties.

Layer	Unit weight (kN/m^3)	Young's modulus (MPa)	Poisson's ratio	Cohesion (kPa)	Friction angle (°)
Expansive soil	19.5	11	0.33	12	17
Clay	21	29	0.3	29	24

slope was set as a free permeable surface, while the bottom surface and the vertical surfaces on both sides of the model were set as impervious water surfaces.

The seepage characteristics of expansive soil slope under rainfall infiltration was calculated under the action of transient flow. For the initial hydraulic state, the model had a pressure head of 0 at the groundwater level. The pressure water head below the underground water level was calculated according to **Eq. 1** and linearly increased with the depth. The unsaturated zone above the underground waterline was evaluated according to the negative pressure head, which decreased linearly in the opposite direction of gravity. The initial water content was considered as the saturated water content below the groundwater level, and the water content in the unsaturated area above the groundwater level decreased gradually with the increase of elevation.

$$p = \gamma h \tag{1}$$

where p stands for the hydraulic head; γ stands for the unit weight of water; h stands for the liquid height.

The Van-Genuchten model is a commonly used model for predicting the soil water characteristic curve of expansive soil, as shown in **Eq. 2**. The model is widely used in the unsaturated seepage analysis of subgrade slope because its parameters are easy to obtain, and it's fitting accuracy is high. The permeability coefficient of expansive soil was measured by the double-loop water-permeation test. According to Darcy's law, permeability coefficient K was calculated using **Eq. 3**. Therefore, the permeability coefficient of the lower clay is 1.90×10^{-8} m/s, while that of expansive soil is 2.70×10^{-7} m/s.

$$\theta = \theta_r + \frac{\theta_s - \theta_r}{[1 + (au_w)^n]^m} \tag{2}$$

$$K = Q/AI \tag{3}$$

where θ, θ_s, and θ_r represent the volume water content, saturated volume water content, and residual volume water content, respectively; u_w represents the pore water pressure; a, n, and m are fitting parameters; K is the permeability coefficient; Q is the water flow of the steady seepage; A is the area of inner diameter of double ring; I represents the hydraulic gradient.

The seepage characteristics of an expansive soil slope under rainfall infiltration are closely related to rainfall intensity, rainfall duration, and rainfall type. According to the meteorological data, rainstorm generally occurs in Nanning from April to August, and the duration is usually 1–2 days. In addition, the duration of moderate rain is approximately 5 days, and its rainfall intensity is 10–25 mm/day. By conversion, the permeability coefficient of expansive soil is approximately 23 mm/day. Considering the boundary condition of rainfall, this study only analyzed the
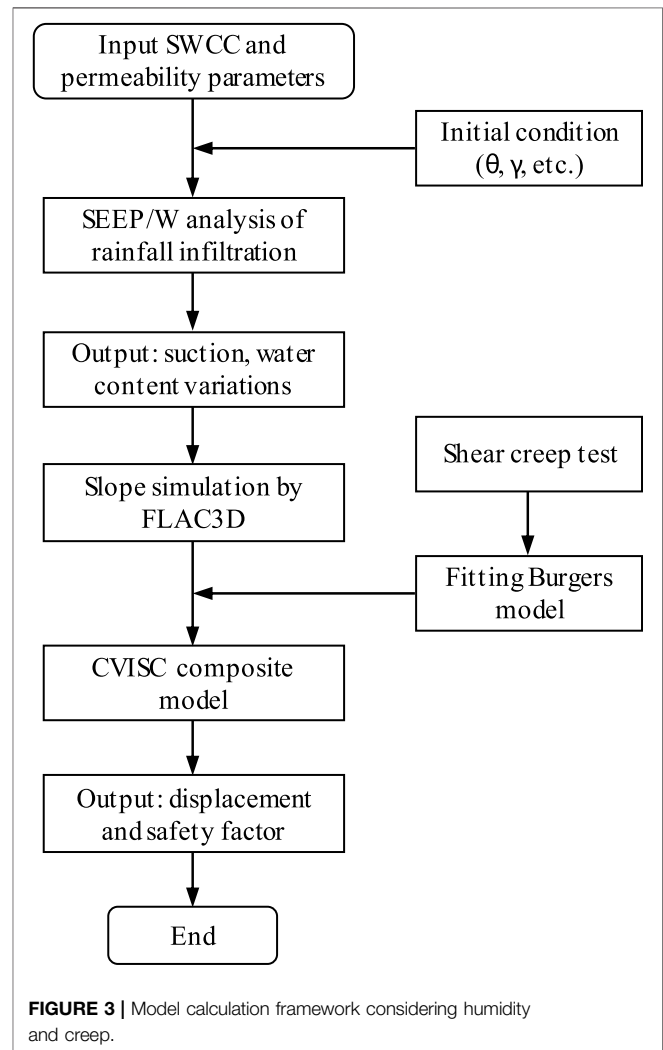
FIGURE 3 | Model calculation framework considering humidity and creep.

seepage condition of the slope under moderate rain. Therefore, the rainfall intensity was set to 10, 12.5, and 20 mm/day, and the rainfall duration was set to 5 days.

3.3 Analysis Plan of Slope Stability

Pore water and gas coexist in unsaturated soil, so the stress of soil is borne by the main framework, the pore water, and the pore gas. According to the extended Mohr-Coulomb criterion, the shear strength (τ_f) of unsaturated soil is expressed as **Eq. 4**. In unsaturated soils, the pore water pressure (u_w) increases, and the matric suction (u_a-u_w) decreases with the increase of the soil water content, and the shear strength (τ_f) of unsaturated soils finally decreases. The cohesion and internal friction angle of
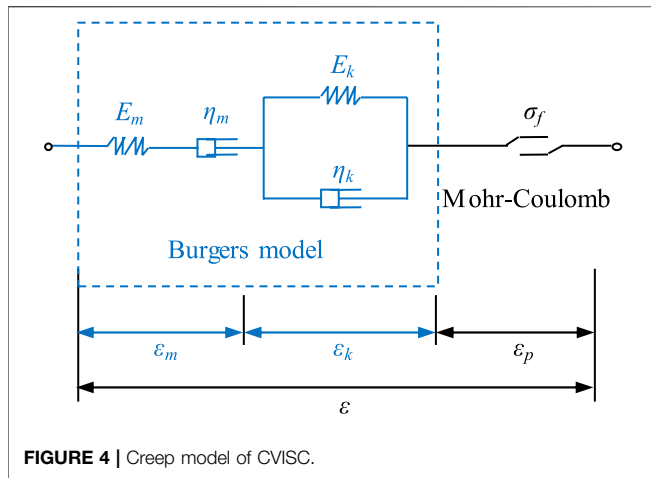
FIGURE 4 | Creep model of CVISC.

expansive soil in the saturated state were 8 kPa and 11°, respectively. The cohesive force and internal friction angle of the lower clay were 27 kPa and 23°, respectively. The matric suction of the unsaturated expansive soil slope changed constantly during rainfall. Therefore, the safety factor and sliding surface of the expansive soil slope also changed dynamically with time during the entire rainfall process.

$$\tau_f = c' + (\sigma_f - u_a)\tan\varphi' + (u_a - u_w)\tan\varphi^b \quad (4)$$

where c' and φ' stand for the effective cohesion and the effective friction angle when the matric suction is 0; σ_f is the yield stress; φ^b is the friction angle related to the matric suction.

To analyze the impact of rainfall conditions on slope stability, the pore water pressure at any moment of the Geo-Studio software was imported into the FLAC3D model in this study. With and without setting the CVISC creep model, the change of the sliding surface of the slope was simulated. Meanwhile, the strength reduction method was used to calculate the safety factor of the expansive soil slope during rainfall infiltration. The calculation flow chart of the stability analysis is shown in **Figure 3**.

The CVISC composite creep model is embedded in the FLAC3D software. This model combines the Burgers and Mohr–Coulomb models, as shown in **Figure 4**. The Burgers model can reflect the viscoelastic deformation of expansive soil well, and the corresponding constitutive relationship is shown in **Eq. 5**. On the basis of the direct shear creep test results and the regression analysis of the creep parameters of the Burgers model, the corresponding model parameters can be obtained.

$$\varepsilon = \frac{\tau}{E_m} + \frac{\tau}{\eta_m}t + \frac{\tau}{E_k}\left(1 - e^{-\frac{E_k}{\eta_k}}\right) \quad (5)$$

where E_m and η_m represent the elastic modulus and the viscosity coefficient of the Maxwell element; E_k and η_k stand for the elastic modulus and the viscosity coefficient of the Kelvin element; τ is the shear stress; ε is the strain; t is the time.

4 RESULTS AND DISCUSSION

The results and their applications are presented and discussed in this section. The Van-Genuchten model used to fit the SWCC of expansive soil is reported in this study, and the effects of stress and compactness on the SWCC of expansive soil were analyzed. Subsequently, the Burgers model was used to study the creep behavior of expansive soils to evaluate the effect of the stress states on the creep properties. Finally, the influence of the above test results on the stability of the expansive soil slope under rainfall conditions is described by numerical analysis.

4.1 SWCC and Fitting Model

To predict the SWCC law of unsaturated expansive soils, some mathematical equations are proposed to obtain the water content or matric suction of soil at any state. **Table 5** shows the fitting parameters of the Van-Genuchten model corresponding to each compaction degree and vertical stress condition, which can be used to understand the water holding capacity of expansive soil. The least square method achieved the best fit for each set of measurement data points and produced different parameter sets. The Van-Genuchten model used the residual water content as a fitting parameter ranging from 0.001 to 0.01. However, these values do not show a uniform trend with stress and density. Generally, the residual water content of the soil sample decreased with the increase of compactness because the high-density soil sample has few pores. Similar conclusions were drawn by Pooni et al. (2021). In addition, according to the results in **Table 5**, the sum of the residual squares of the fitted data is greater than 99%, indicating that the Van-Genuchten model can effectively predict the SWCC of expansive soil. The numerical simulation used 85% compacting degree and 0 kPa vertical pressure.

Figure 5 shows the SWCC test results in different states. The experimental results show that the SWCC of unsaturated expansive soil had an obvious turning point, which can clearly reflect the boundary effect and transition stages. When the matric suction was less than 50 kPa, the soil sample was in the boundary effect stage. In this stage, the water content of the soil sample decreased slowly with the increase of the matric suction, and the curve is gentle. The gas phase in the soil was suspended in the water as a closed bubble and flowed with water because the soil was near saturation. When the suction exceeded 50 kPa until the end of the test, the soil sample was in the transition stage. At this stage, the SWCC exhibited approximately linear changes. The water content of the soil samples decreased clearly with the increase of the matric suction. At this stage, the gas phase of the soil was partially connected with the internal pores, and the air began to enter the soil and occupy the large pore channels in the soil. Therefore, the saturation decreased rapidly with the increase of the suction, and the soil properties changed sharply. In practical engineering, this stage is characterized by unsaturated expansive soil.

Figure 5A shows the test results on expansive soil under no overburden pressure. Under the same matric suction conditions, the higher the dry density was, the lower the water content was; the effect of dry density on matric suction weakened when the matric suction increased gradually. This phenomenon occurred

TABLE 5 | Fitting parameters for SWCC.

Compaction degree (%)	Vertical stress (kPa)	a (kPa)	n (E)	M	θ_r (%)	R^2 (%)
85	0	1.196-2	1.851	0.460	1.84-3	99.75
	30	1.613-2	1.890	0.471	2.74-3	99.61
	60	1.541-2	1.978	0.494	1.77-3	99.56
	90	1.493-2	2.014	0.503	1.25-3	99.43
90	0	1.298-2	1.882	0.469	1.75-3	99.61
	30	1.196-2	1.924	0.480	2.25-3	99.56
	60	1.128-2	2.014	0.504	1.44-3	99.50
	90	1.139-2	2.053	0.513	1.04-3	99.55
98	0	1.107-2	2.011	0.503	1.60-3	99.54
	30	1.081-2	2.079	0.519	2.24-3	99.38
	60	1.056-2	2.184	0.542	4.85-3	99.48
	90	1.135-2	2.219	0.549	1.38-3	99.42
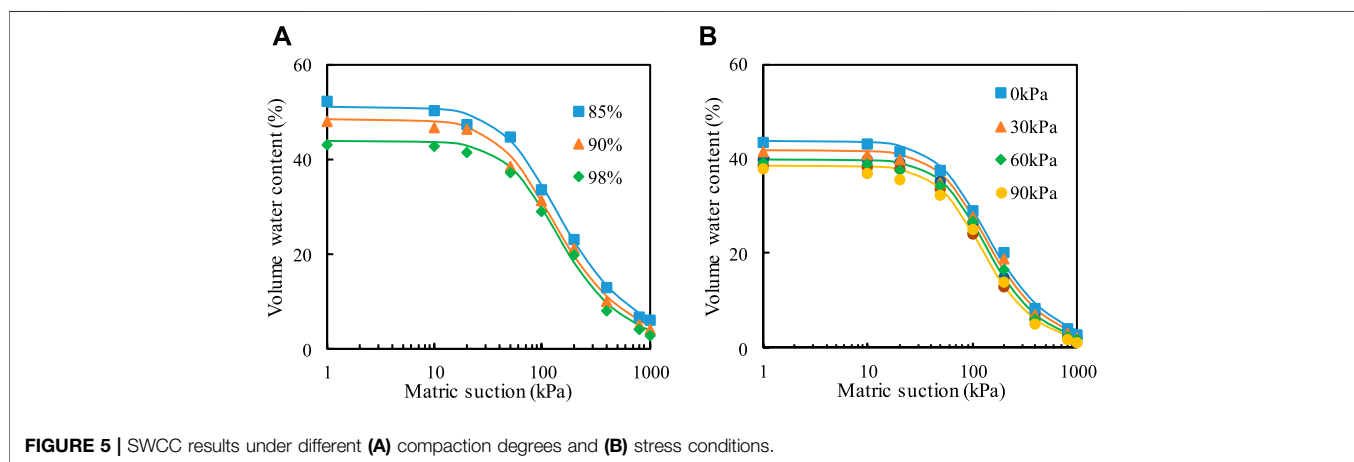
FIGURE 5 | SWCC results under different **(A)** compaction degrees and **(B)** stress conditions.

because the effect of dry density on the soil–water characteristic curve was mainly realized by changing the pore condition of the soil. When the dry density was small, the internal pores and pore size of the expansive soil were large, resulting in poor water holding capacity. **Figure 5B** shows the SWCC of the soil sample with 98% compaction degree. The results show that the air intake of the soil samples moved back, and the influence of suction on the water content weakened with the increase of vertical stress. Similarly, the greater the vertical stress was, the lesser the porosity of the soil sample and the greater the capillary suction of the soil were.

4.2 Direct Shear Creep Results

Figure 6 displays the shear strain time relationship curve of the graded loading. The compaction degree of the testing soil was 85%. The results under the vertical stress of 50 and 100 kPa show that when the deviator stress level was low, the strain of the expansive soil only included instantaneous strain and attenuated creep strain during the test duration; when the deviator stress increased to 93.5 kPa, the creep process of expansive soil experienced three complete stages during the test time, namely, attenuation creep, steady-state creep, and accelerated creep, and the expansive soil finally underwent creep failure;

when horizontal shear stress was added to 161.5 kPa, the two soil samples were suddenly damaged, so the results are not shown in the figure. When the vertical stress was 200 and 300 kPa, the creep curve of soil showed the same change trend. When the horizontal shear stress was less than 42.5 kPa, attenuation creep was observed, the shear displacement was mainly instantaneous, and the creep tended to be stable within 2 days. The change process of the creep curve is consistent with the creep law when the vertical stress is 50 and 100 kPa.

Traditional rheological model theory regards the soil as a linear body and uses linear rheological theory to study the rheological problem of soil. The linear creep model shows a linear relationship between strain and stress when subjected to external stress. However, many studies now believe that the constitutive relationship of soil is different at different times and strain increases nonlinearly. For the nonlinear creep model, the stress–strain relationship is viscoelastic. On the basis of the direct shear creep test data, regression analysis was performed on the parameters of the Burgers model. The results in **Table 6** indicate that the fitting effect of the model is better under high vertical stress. In general, this model can be used to describe the nonlinear creep behavior of expansive soil under different stress states and has certain applicability.
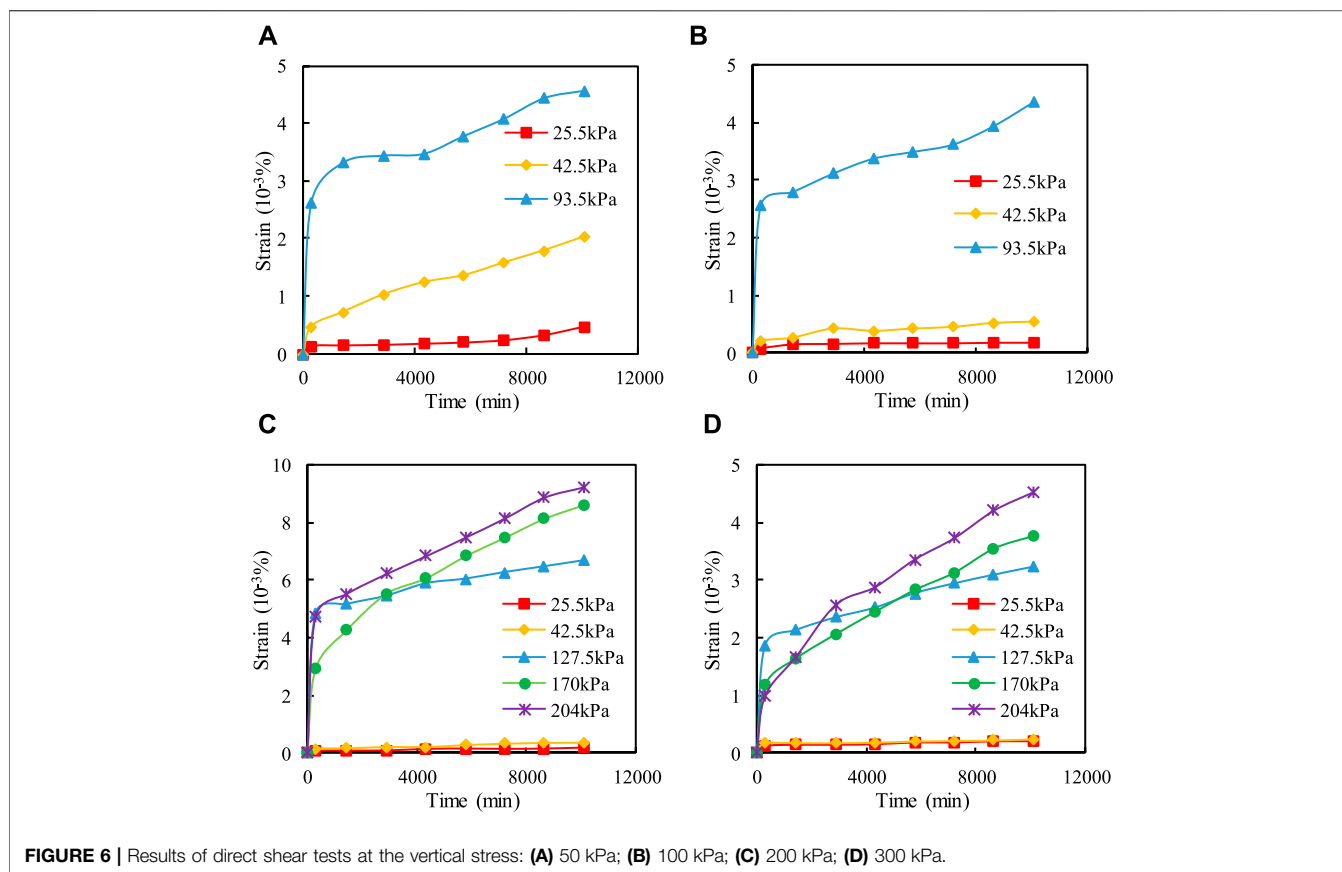
FIGURE 6 | Results of direct shear tests at the vertical stress: **(A)** 50 kPa; **(B)** 100 kPa; **(C)** 200 kPa; **(D)** 300 kPa.

TABLE 6 | Fitting parameters of Burgers model.

| Vertical stress (kPa)	Shear stress (kPa)	E_m (kPa)	E_k (kPa)	η_{lm} (kPa·min)	η_k (kPa·min)	R^2 (%)
50	25.5	2.80E + 05	1.50E + 05	4.56E + 09	1.63E + 08	88.54
	42.5	4.25E + 05	4.25E + 04	5.94E + 08	4.25E + 07	93.49
	93.5	9.35E + 05	9.35E + 04	2.22E + 08	9.35E + 07	80.23
100	25.5	2.98E + 08	1.77E + 05	9.59E + 09	8.25E + 07	99.84
	42.5	4.72E + 08	1.57E + 05	1.56E + 09	3.91E + 07	96.62
	93.5	1.04E + 09	3.62E + 04	5.70E + 08	3.02E + 06	99.60
200	25.5	2.83E + 08	5.26E + 05	2.63E + 09	4.43E + 07	93.53
	42.5	4.70E + 08	3.50E + 05	1.70E + 09	8.44E + 06	98.37
	127.5	1.45E + 09	2.60E + 04	6.89E + 08	4.37E + 05	99.82
	170	1.94E + 09	4.96E + 04	3.07E + 08	8.35E + 05	98.38
	204	2.33E + 09	4.25E + 04	4.43E + 08	7.15E + 05	99.83
300	25.5	2.82E + 08	2.26E + 05	3.12E + 09	2.22E + 07	98.87
	42.5	4.90E + 08	2.70E + 05	5.71E + 09	4.55E + 06	99.12
	127.5	1.45E + 09	6.67E + 04	9.26E + 08	1.12E + 06	99.72
	170	1.94E + 09	1.37E + 05	6.46E + 08	2.31E + 06	99.54
	204	2.33E + 09	1.67E + 05	5.86E + 08	2.80E + 06	98.24

4.3 Seepage Analysis Subjected to Rainfall Infiltration

The process of rainfall infiltration was simulated by the Geo-studio/Seep software. **Figure 7** shows the slope humidity field at different rainfall times, subjected by the rainfall intensity of 20 mm/day. In the model, the moisture content of the soil increased gradually with continuous rainfall. The shallower the depth was, the earlier the start of water content increase was. The influence of rainfall infiltration on the soil moisture content of the slope gradually developed from the surface soil to its depth. The
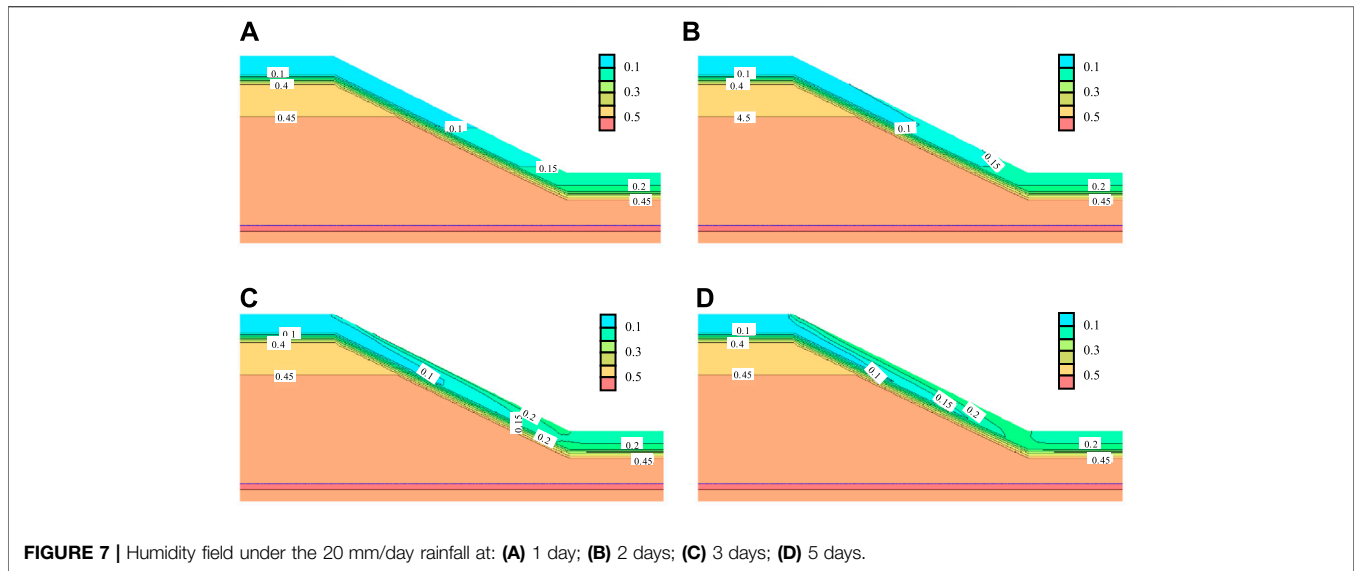
FIGURE 7 | Humidity field under the 20 mm/day rainfall at: **(A)** 1 day; **(B)** 2 days; **(C)** 3 days; **(D)** 5 days.
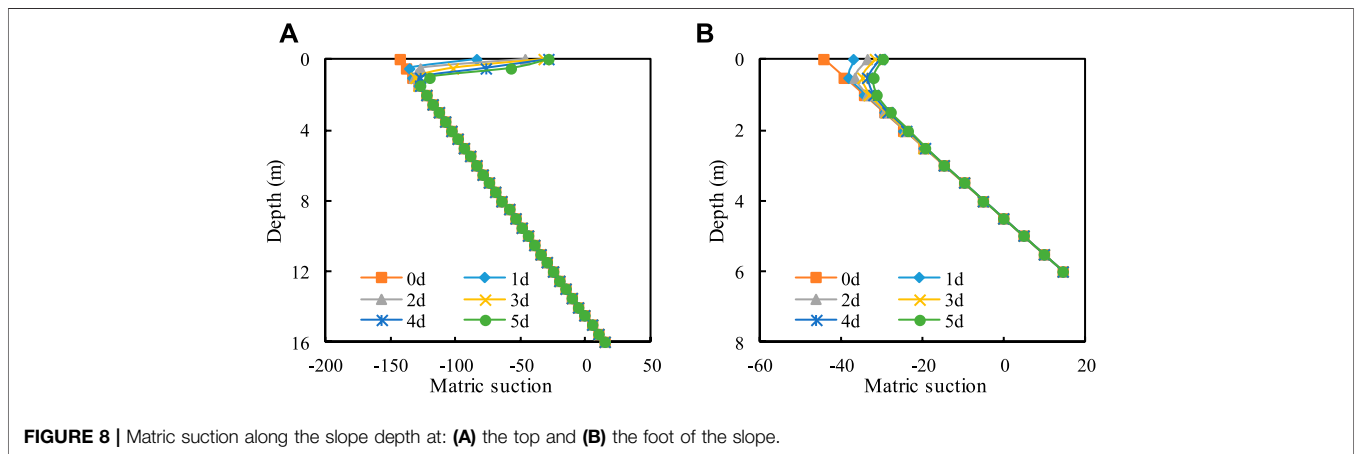
FIGURE 8 | Matric suction along the slope depth at: **(A)** the top and **(B)** the foot of the slope.

influence of the depth of rainfall infiltration gradually increased with the rainfall duration, and the nearer the slope was, the greater the increase in water content was. After the rainfall, the water content in the expansive soil was replenished by rain and infiltrated along the slope. Given the poor permeability of clay, the rainfall only gathered above the slope foot when the rainfall lasted for 3 days.

The unsaturated seepage process of expansive soil was accompanied by the change in matric suction. **Figure 8** shows the suction variation along the depth at the foot and top of the slope during rainfall, according to the above distribution of water content. The results show that the matric suction changes obviously in the expansive soil but has no effect on the ordinary clay. A positive correlation existed between the range of suction and the depth of rainfall infiltration because the rainfall intensity was greater than the soil infiltration capacity. Meanwhile, the matric suction of the expansive soil near the top of the slope was significantly higher than that near the foot of the slope.

4.4 Influence of Rainfall Infiltration on Slope Stability

The matric suction of soil changes constantly with rainfall, and also affects the shear properties of expansive soil slope. As it displayed in **Figure 3**, the computation results of the humidity were obtained by the Geo-studio model and were imported into the slope model in the FLAC3D. **Figures 9A**, **10A** are the distributions of pore water pressure before and after the rainfall. In the initial state, the pore water pressure presents gradient changes along the gravity direction. After the rainfall for 5 days, the pore water pressure increased within a certain region in the slope, which was related to the influence depth of rainfall infiltration.

The increase in humidity led to the strength softening of expansive soil, which affected the shear strain and displacement of the slope. **Figures 9B**, **10B** illustrate the effect of the rainfall infiltration on the slope stability. As the rain occurred, the maximum shear surface of the slope moved down and the sliding speed increased at the foot of the slope. Meanwhile, the
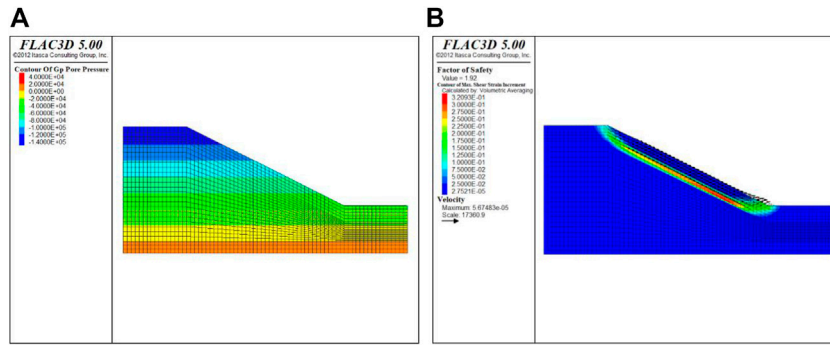
FIGURE 9 | Distribution of **(A)** pore water pressure and **(B)** shear strain after reduction (T = 0 days).
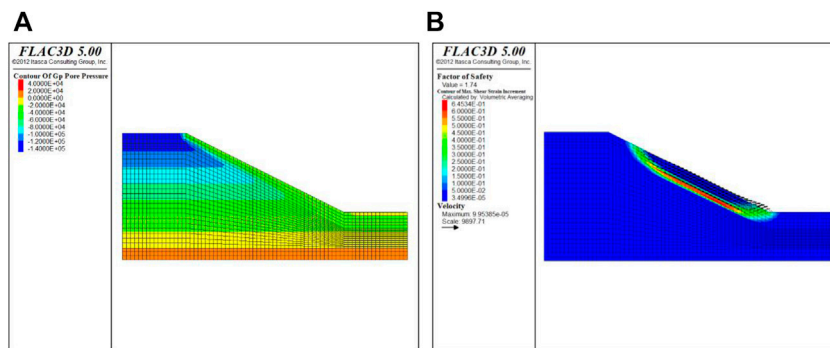

FIGURE 10 | Distribution of **(A)** pore water pressure and **(B)** shear strain after reduction (T = 5 days).
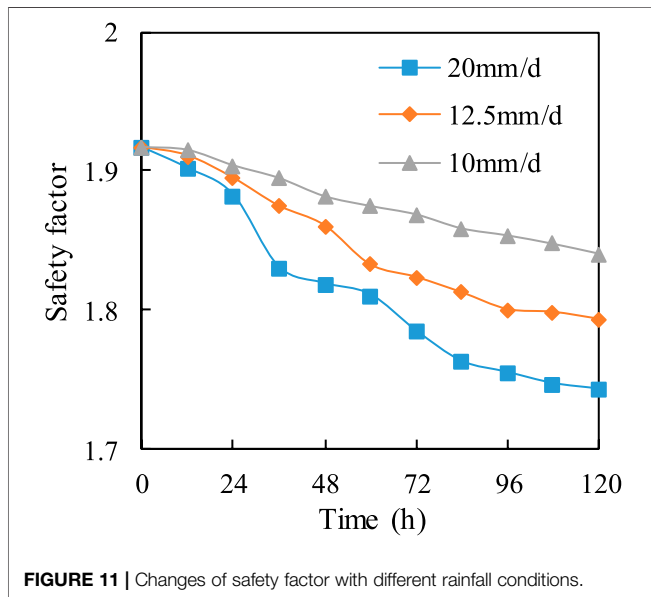

FIGURE 11 | Changes of safety factor with different rainfall conditions.

the slope was gradually losing stability. **Figure 11** shows the change in the safety factor of the expansive soil slope under different rainfall conditions. the higher the rainfall intensity was, the higher the rainfall infiltration rate and the deeper the rainfall infiltration were. With the increase of rainfall intensity under the same infiltration rate, the more water infiltrating the soil was, the faster the soil water content increase was.

4.5 Influence of Creep Behavior on Slope Stability

Furthermore, the long-term performance of the slope is related to the creep process of expansive soil, which may last for months or years. Based on the CVISC model, the viscoelastic-plastic deformation of the expansive slope was calculated in the above simulation. **Figure 12** shows the contours of the horizontal displacement during different creep times. The model was in a naturel water distribution, as shown in **Figure 9A**. On the one hand, the displacement of the slope increased obviously over time and the maximum displacement occurred at the foot of the slope. On the other hand, the deformation within the clay layer was at a low level with the time, due to no assignment of the creep model for it.

According to the stability analysis, the expansive soil slope can easily slip along the horizontal direction at the foot of the slope.
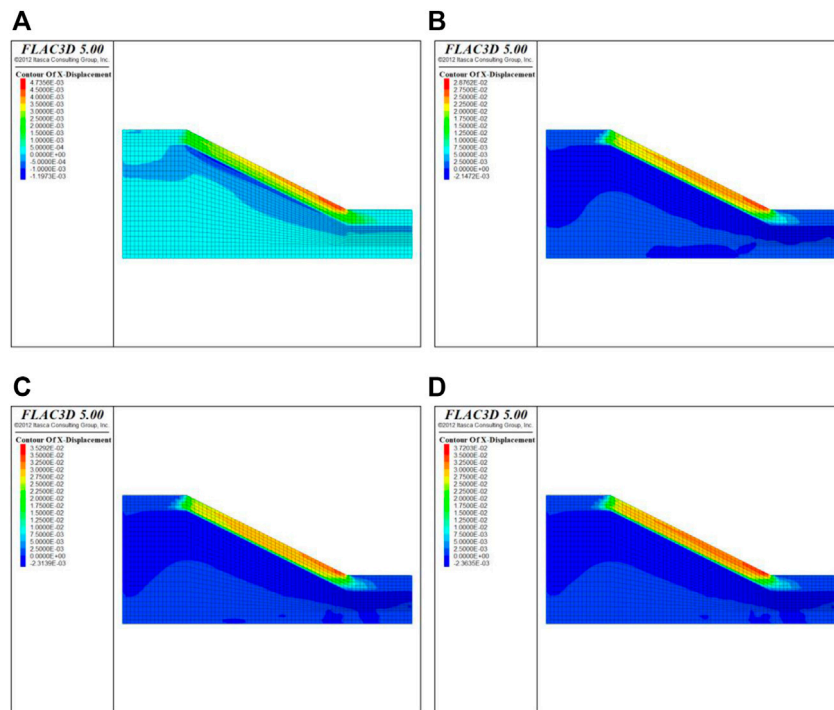
safety factor of stability analysis decreased from the initial value of 1.917 to 1.743. It was seen clearly that the seepage formed near the slope surface and flowed to the foot of the slope. As a result, the most dangerous sliding surface moved to the foot of the slope, and

FIGURE 12 | Changes of x-displacement of slope at: **(A)** 1 year; **(B)** 3 years; **(C)** 5 years; **(D)** 7 years.
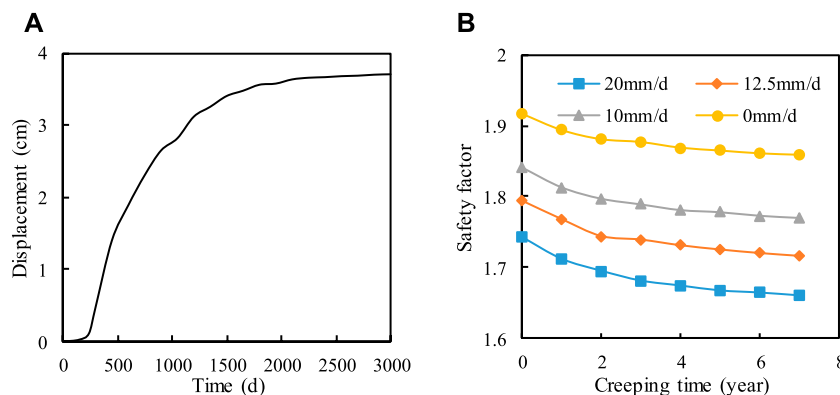

FIGURE 13 | Changes of **(A)** displacement of the slope foot and **(B)** safety factor of expansive soil slope.

Therefore, **Figure 13A** shows the change of horizontal displacement at the foot of the slope with time was measured in the above model. It did not take the rainfall into account. The test results show that the horizontal displacement of the slope foot gradually increased with the extension of time. The displacement increased greatly in 1–3 years, but the creep was stable after 7 years. The maximum displacement was approximately 3.69 cm. Meanwhile, the long-term creep behavior also led to slope stability attenuation. However, compared with the creep failure of the expansive soil, the rainfall infiltration is a rapid and significant effect on the stability of the slope. **Figure 13B**

shows safety factors of the slope considering the rainfall of 5 days after the long-term creep process. The result in the absence of rainfall shows that the slope safety factor decreased from 1.917 to 1.859, while the time increased from 0 to 7 years. The occurrence of rainfall further accelerated the failure of the slope because the wetting of the slope reduced the maximum strength of the slope. For 5 days suffered by 20 mm/d rainfall, the safety factor reduced 0.083 over time. For no rainfall, the safety factor only decreased 0.058. It implies that the influence of the creep behavior on the slope stability was also enhanced with the increase of rainfall intensity.

4.6 Discussion

The analyses have shown that the rainfall and the creep behavior are significant over time that is related to the stability of the expansive soil slope. Previous studies suggested that the depth of rainfall infiltration ranged from 1.0 to 3.5 m, and it was possible to occur a passive failure within the softened soil layer at shallow depths (Zhan et al., 2007; Pei et al., 2020). The increase in water content was detrimental for the slope stability of the unsaturated soil, as it mentioned in **Eq. 4**. Furthermore, the creep deformation exacerbated the failure process of the unsaturated slope. In this study, the effects of the stress state on the SWCC and creep properties were obtained at laboratory. The corresponding models and parameters were assigned into the slope simulation. The ranges of matric suction were positively correlated with the depth of rainfall infiltration. This was consistent with the filed results reported by Wang et al. (2017), who found that the displacement of the slope was mainly along the horizontal direction and the deformation rate depended on the rainfall intensity and duration.

The numerical model was considering the long-term creep deformance of the slope. The result shows that there was a period of rapid growth in the horizontal displacement at the slope foot. Besides, the occurrence of rainfall may accelerate this failure of the slope. Therefore, the creep behavior of the expansive soil slope could be under-estimated in the slope design. Further study should be carried out to investigate the effect of the long-term creep on micro-cracks and hydraulic properties of the expansive soil. In addition, the current study only analyzed the effect of the rainfall on the slope stability before and after the creep process, and further study should consider both dry-wet cycles and creep time of this investigated soil on the slope deformation. At last, some treatment and modified soil should be applied to further consider the effects of rainfall and creep on SWCC and slope stability, including the soil-rock mixture (Yao et al., 2022).

5 CONCLUSION

This study investigated the effect of the rainfall infiltration on the stability of the expansive soil slope before and after long-term creep proceed. Experimental tests were performed to obtain the SWCC and creep behavior of the unsaturated expansive soil. A pressure plate apparatus was used to measure the SWCCs of different compaction degrees and stress conditions. Meanwhile, the Burgers model was applied to describe the creep behavior under different stress conditions. Both Geo-studio software and FLAC3D were combined to calculate the stability of the expansive soil slope under rainfall infiltration. The main findings of this paper were presented as following.

(1) The Van-Genuchten model had a good fitting effect with the results of SWCC. For the SWCC, there was an obvious turning point, distinguishing between the boundary effect stage and the transition stage. As the compaction degree or the vertical stress increased, it presents a general trend with a lower desorption rate in the SWCC.

(2) The nonlinearity of the creep behavior was affected by creep time and stress level on the expansive soil. The longer the creep time and the higher the stress level, the higher the nonlinear degree. The fitting results show that the Burgers model can be used to characterize the creep behavior of expansive soil.

(3) Rainfall infiltration has a great influence on the stability of the expansive soil slope. With the increase of rainfall time, the safety factor decreased gradually. Meanwhile, the most dangerous slide of the slope moves towards the foot of the slope.

(4) The preliminary analyses have shown that there was a period of rapid growth in the horizontal displacement at the slope foot, considering the long-term creep model. This phenomenon could reduce the slope stability. Besides, its influence on the safety factor was further enhanced with the increase of rainfall intensity.

DATA AVAILABILITY STATEMENT

The original contributions presented in the study are included in the article/supplementary material, further inquiries can be directed to the corresponding author.

AUTHOR CONTRIBUTIONS

All authors listed have made a substantial, direct, and intellectual contribution to the work and approved it for publication.

REFERENCES

Cong, S., Nie, Z., and Hu, Q. (2020). A Disturbed State Concept-Based Stress-Relaxation Model for Expansive Soil Exposed to Freeze-Thaw Cycling. *KSCE J. Civ Eng.* 24 (9), 2621–2630. doi:10.1007/s12205-020-2000-3

Dai, Z., Chen, S., and Li, J. (2020). Physical Model Test of Seepage and Deformation Characteristics of Shallow Expansive Soil Slope. *Bull. Eng. Geol. Environ.* 79 (8), 4063–4078. doi:10.1007/s10064-020-01811-0

Fan, Z., Xiao, H., and Tang, Y. (2011). Experimental Study on Creep Characteristics for Nanning Unsaturated Expansive Soils. *Highw. Eng.* 36 (6), 43–47. doi:10.3969/j.issn.1674-0610.2011.06.009

Fredlund, D. G., and Xing, A. (1994). Equations for the Soil-Water Characteristic Curve. *Can. Geotech. J.* 31 (4), 521–532. doi:10.1139/t94-061

Gardener, W., Hillel, D., and Benzamin, Y. (1970). Post Irrigation Movement of Soil Water: II. Simultaneous Redistribution and Evaporation. *Water Resour. Res.* 6 (4), 1148–1153.

Hou, F., Lai, Y., Liu, E., Luo, H., and Liu, X. (2018). A Creep Constitutive Model for Frozen Soils with Different Contents of Coarse Grains. *Cold Regions Sci. Tech.* 145, 119–126. doi:10.1016/j.coldregions.2017.10.013

Houston, S. L., Houston, W. N., and Wagner, A.-M. (1994). Laboratory Filter Paper Suction Measurements. *Geotechnical Test. J.* 17 (2), 185–194.

Huang, W., Wen, K., Deng, X., Li, J., Jiang, Z., Li, Y., et al. (2020). Constitutive Model of Lateral Unloading Creep of Soft Soil under Excess Pore Water Pressure. *Math. Probl. Eng.* 2020, 1-13. doi:10.1155/2020/5017546

Ikeagwuani, C. C., and Nwonu, D. C. (2019). Emerging Trends in Expansive Soil Stabilisation: A Review. *J. Rock Mech. Geotechnical Eng.* 11 (2), 423–440. doi:10.1016/j.jrmge.2018.08.013

Jalal, F. E., Xu, Y., Jamhiri, B., and Memon, S. A. (2020). On the Recent Trends in Expansive Soil Stabilization Using Calcium-Based Stabilizer Materials (CSMs): A Comprehensive Review. *Adv. Mater. Sci. Eng.* 2020, 1-23. doi:10.1155/2020/1510969

Khan, M. A., Wang, J. X., and Sarker, D. (2020). Development of Analytic Method for Computing Expansive Soil-Induced Stresses in Highway Pavement. *Int. J. Geomech.* 20 (2), 04019160. doi:10.1061/(asce)gm.1943-5622.0001511

Leng, T., Tang, C., Xu, D., Li, Y., Zhang, Y., Wang, K., et al. (2018). Advance on the Engineering Geological Characteristics of Expansive Soil. *J. Eng. Geology.* 26 (1), 112–128.

Li, D., Yang, X., and Chen, J. (2017). A Study of Triaxial Creep Test and Yield Criterion of Artificial Frozen Soil under Unloading Stress Paths. *Cold Regions Sci. Tech.* 141, 163–170. doi:10.1016/j.coldregions.2017.06.009

Li, J., Zheng, J., Yao, Y., Zhang, J., and Peng, J. (2019). Numerical Method of Flexible Pavement Considering Moisture and Stress Sensitivity of Subgrade Soils. *Adv. Civil Eng.* 2019, 1-10. doi:10.1155/2019/7091210

Liu, J., Jing, H., Meng, B., Wang, L., Yang, J., and Zhang, X. (2020). A Four-Element Fractional Creep Model of Weakly Cemented Soft Rock. *Bull. Eng. Geol. Environ.* 79 (10), 5569–5584. doi:10.1007/s10064-020-01869-w

Lu, Y., Liu, S., Alonso, E., Wang, L., Xu, L., Li, Z., et al. (2019). Volume Changes and Mechanical Degradation of a Compacted Expansive Soil under Freeze-Thaw Cycles. *Cold Regions Sci. Tech.* 157, 206–214. doi:10.1016/j.coldregions.2018.10.008

Mehta, B., Sachan, A., and Engineering, G. (2017). Effect of Mineralogical Properties of Expansive Soil on its Mechanical Behavior. *Geotech Geol. Eng.* 35 (6), 2923–2934. doi:10.1007/s10706-017-0289-6

Pawlik, Ł., and Šamonil, P. (2018). Soil Creep: The Driving Factors, Evidence and Significance for Biogeomorphic and Pedogenic Domains and Systems - A Critical Literature Review. *Earth-Science Rev.* 178, 257–278. doi:10.1016/j.earscirev.2018.01.008

Pei, P., Zhao, Y., Ni, P., and Mei, G. (2020). A Protective Measure for Expansive Soil Slopes Based on Moisture Content Control. *Eng. Geology.* 269, 105527. doi:10.1016/j.enggeo.2020.105527

Peng, R., Peng, W., Hua, Z., and Yin, T. (2020). Nonlinear Behavior of clay Creep and its Fractional Derivative Creep Model. *Eng. Mech.* 37 (9), 153–160. doi:10.6052/j.issn.1000-4750.2019.10.0624

Pooni, J., Robert, D., Giustozzi, F., Gunasekara, C., Setunge, S., and Venkatesan, S. (2021). Hydraulic Characteristics of Stabilised Expansive Subgrade Soils in Road Pavements. *Int. J. Pavement Eng.*, 1–18. doi:10.1080/10298436.2021.1883610

Shan, R.-l., Bai, Y., Ju, Y., Han, T.-y., Dou, H.-y., and Li, Z.-l. (2021). Study on the Triaxial Unloading Creep Mechanical Properties and Damage Constitutive Model of Red sandstone Containing a Single Ice-Filled Flaw. *Rock Mech. Rock Eng.* 54 (2), 833–855. doi:10.1007/s00603-020-02274-1

Soltani, A., Deng, A., and Taheri, A. (2018). Swell-compression Characteristics of a Fiber-Reinforced Expansive Soil. *Geotextiles and Geomembranes* 46 (2), 183–189. doi:10.1016/j.geotexmem.2017.11.009

Take, W. A., and Bolton, M. D. (2003). Tensiometer Saturation and the Reliable Measurement of Soil Suction. *Géotechnique* 53 (2), 159–172. doi:10.1680/geot.2003.53.2.159

Toll, D. G., Lourenço, S. D. N., and Mendes, J. (2013). Advances in Suction Measurements Using High Suction Tensiometers. *Eng. Geology.* 165, 29–37. doi:10.1016/j.enggeo.2012.04.013

Van Genuchten, M. T. (1980). A Closed-form Equation for Predicting the Hydraulic Conductivity of Unsaturated Soils. *Soil Sci. Soc. America J.* 44 (5), 892–898. doi:10.2136/sssaj1980.03615995004400050002x

Wang, J., Gu, T., and Xu, Y. (2017). Field Tests of Expansive Soil Embankment Slope Deformation under the Effect of the Rainfall Evaporation Cycle. *Appl. Ecol. Env Res.* 15 (3), 343–357. doi:10.15666/aeer/1503_343357

Wang, M., Kong, L., Zang, M., and Engineering, G. (2015). Effects of Sample Dimensions and Shapes on Measuring Soil-Water Characteristic Curves Using Pressure Plate. *J. Rock Mech. Geotechnical Eng.* 7 (4), 463–468. doi:10.1016/j.jrmge.2015.01.002

Yang, G., and Bai, B. (2019). Thermo-hydro-mechanical Model for Unsaturated clay Soils Based on Granular Solid Hydrodynamics Theory. *Int. J. Geomech.* 19 (10), 04019115. doi:10.1061/(asce)gm.1943-5622.0001498

Yao, Y., Li, J., Ni, J., Liang, C., and Zhang, A. (2022). Effects of Gravel Content and Shape on Shear Behaviour of Soil-Rock Mixture: Experiment and DEM Modelling. *Comput. Geotechnics* 141, 104476. doi:10.1016/j.compgeo.2021.104476

Yao, Y., Ni, J., and Li, J. (2021). Stress-dependent Water Retention of Granite Residual Soil and its Implications for Ground Settlement. *Comput. Geotechnics* 129, 103835. doi:10.1016/j.compgeo.2020.103835

Yao, Y., Qian, J., Li, J., Zhang, A., and Peng, J. (2019). Calculation and Control Methods for Equivalent Resilient Modulus of Subgrade Based on Nonuniform Distribution of Stress. *Adv. Civil Eng.* 2019, 1-11. doi:10.1155/2019/6809510

Yao, Y., Zheng, J., Zhang, J., Peng, J., and Li, J. (2018). Model for Predicting Resilient Modulus of Unsaturated Subgrade Soils in south China. *KSCE J. Civ Eng.* 22 (6), 2089–2098. doi:10.1007/s12205-018-1703-1

Zhan, T. L., Ng, C. W., and Fredlund, D. G. (2007). Field Study of Rainfall Infiltration into a Grassed Unsaturated Expansive Soil Slope. *Can. Geotech. J.* 44 (4), 392–408. doi:10.1139/t07-001

Zhang, J.-h., Li, F., Zeng, L., Zheng, J.-l., Zhang, A.-s., and Zhang, Y.-q. (2020). Effect of Cushion and Cover on Moisture Distribution in clay Embankments in Southern China. *J. Cent. South. Univ.* 27 (7), 1893–1906. doi:10.1007/s11771-020-4418-7

Zhang, J., Li, F., Zeng, L., Peng, J., and Li, J. (2021). Numerical Simulation of the Moisture Migration of Unsaturated clay Embankments in Southern China Considering Stress State. *Bull. Eng. Geol. Environ.* 80 (1), 11–24. doi:10.1007/s10064-020-01916-6

Zheng, Y., Chen, C., Liu, T., and Ren, Z. (2021). A New Method of Assessing the Stability of Anti-dip Bedding Rock Slopes Subjected to Earthquake. *Bull. Eng. Geol. Environ.* 80 (5), 3693–3710. doi:10.1007/s10064-021-02188-4

Zheng, Y., Chen, C., Liu, T., Zhang, H., Xia, K., and Liu, F. (2018). Study on the Mechanisms of Flexural Toppling Failure in Anti-inclined Rock Slopes Using Numerical and Limit Equilibrium Models. *Eng. Geology.* 237, 116–128. doi:10.1016/j.enggeo.2018.02.006

Zhou, F., Wang, L., and Liu, H. (2021). A Fractional Elasto-Viscoplastic Model for Describing Creep Behavior of Soft Soil. *Acta Geotech.* 16 (1), 67–76. doi:10.1007/s11440-020-01008-5